Int. J. Electrochem. Sci., 15 **(2020)** 3013 – 3028, doi: 10.20964/2020.04.54

International Journal of
ELECTROCHEMICAL
SCIENCE
www.electrochemsci.org

Degradation of the Sealing Silicone Rubbers in a Proton Exchange Membrane Fuel Cell at Cold Start Conditions

Fan Wu[1], *Ben Chen*[2,*], *Mu Pan*[1]

[1] State Key Laboratory of Advanced Technology for Materials Synthesis and Processing, Wuhan University of Technology, Wuhan 430070, China
[2] Hubei Key Laboratory of Advanced Technology for Automotive Components, Wuhan University of Technology, Wuhan, 430070, China
[*]E-mail: chenben99@whut.edu.cn

Received: 7 December 2019 / *Accepted:* 12 February 2020 / *Published:* 10 March 2020

The sealing performance of gaskets is important for ensuring successful cold starts and stable operation of proton exchange membrane fuel cells (PEMFCs). To simplify water and thermal management, fuel cells in cars usually operate at an elevated temperature of 90 °C. In this work, the degradation of silicone rubbers, as potential gasket materials for PEMFCs, was investigated in different cold-start processes ranging from -5 °C to 90 °C; -10 °C to 90 °C; and -20 °C to 90 °C. After 200 temperature cycles, the aged silicone rubbers were cut into gaskets and assembled into a PEMFC single cell for assessments of gas leakage. The hardness of the silicone rubbers increased and their weight gradually decreased with increasing number of temperature cycles. In addition, these characteristics deteriorated with decreasing initial cycling temperature. Atomic absorption spectrometry indicated that calcium leached out from the silicone rubbers into the soaking solution. Scanning electron microscopy revealed that cracks and caves formed on the sample surfaces and the attenuated total reflection Fourier transform infrared spectra results showed that the surface chemistry was significantly changed. Importantly, the gas leakage of the PEMFC single cell showed that the sealing performance of the aged silicone rubbers changed significantly compared to that of the pristine rubbers.

Keywords: Silicone rubbers, PEMFC, cold-start process, aging, gas leakage

1. INTRODUCTION

Proton exchange membrane fuel cells (PEMFCs) convert chemical energy from fuel and oxidants directly into electricity and are considered to be a promising alternative energy conversion device. PEMFCs exhibit unique advantages in terms of fast start-up, high power density, efficiency, reliability, quiet operation, environmental-friendliness, and wide range of applications [1-4]. To meet the requirements of commercial application, the cold start ability of PEMFCs is a critical target in fuel cell

technical road maps and the cold start performance has improved significantly in recent years. In addition to the well-known transport phenomena inside PEMFCs, other factors governing cold starting are related to the reliability and stability of components, which suffer from subfreezing at operating temperatures during the cold start process [5-8]. Gaskets installed inside PEMFCs play an important role in segregating hydrogen, air, and coolant, ensuring the reliability and stability for long-term PEMFC operation [9, 10]. Gas leakage caused by sealing failure negatively affects PEMFCs and may cause burning due to reactive gas leakage, especially hydrogen, during operation [11]. In the cold start process, the temperature of the PEMFC increases gradually from subfreezing to approximately ≥80 °C. Gaskets inside the PEMFC suffer from the effects of wide temperature gradients combined with mechanical compressive loads causing thermal stress in the gasket. In addition, gaskets are exposed to acidic environments as well as humidified hydrogen and air, which can easily cause chemical changes in the gasket materials [12-15]. The long-term stability and durability of gaskets are crucial to both sealing and electrochemical performance, directly affecting the service life of PEMFCs.

Because of its low cost, good mechanical properties, and simple manufacturing process, silicone rubber is a potential gasket material for PEMFCs [16, 17]. The performance of silicone rubbers in fuel cell working environments has been investigated previously [18-23]. Li et al. [18, 19] studied the degradation of silicone rubbers when exposed to simulated and accelerated PEMFC environments at 70 °C, demonstrating that the acid concentration of test solutions significantly affected the degradation of silicone rubber samples. Chang et al. [24] studied silicone rubber aging with samples of different hardness values subjected to dry and humidified air at 80 °C. The authors showed that the water molecules in the humidified gases can accelerate silicone rubber aging due to the chemical decomposition of cross-linker units connecting polysiloxane backbones and of methyl groups attached to silicon. Feng et al. [25] studied the degradation of silicone rubbers with different hardness values in various aqueous solutions at 80 °C. The authors demonstrated that the durability of silicone rubbers was enhanced with increasing hardness. Tan et al. [26-30] investigated the degradation of silicone rubbers subjected to a constant PEMFC compressive load on the seals and soaked in a simulated PEMFC environment at 60 °C and 80 °C, resulting in significantly altered mechanical properties of the silicone rubber material. In addition, with increasing temperature and acid concentration, the tested silicone rubbers degraded more rapidly. The degradation of silicone rubbers originated from the chemical decomposition of the silicon-based backbone accompanied by the filler leaching. Clarke et al. [31] compared the accelerated aging of silicone rubber gasket material in PEMFC environments at its working and elevated temperatures (140 °C). Their analysis showed that acid hydrolysis was the most common mechanism of silicone rubber degradation and similar degradation occurred under both real fuel cell and under accelerated aging conditions. Cui et al. [32, 33] studied the sealing force and thermal stress development of silicone rubbers under two temperature cycles, between 40 °C and 70 °C and between – 10 °C and 40 °C. The sealing force development during startup, operation, and shutdown periods of a PEMFC stack was also measured. The authors demonstrated that thermal expansion or contraction of the silicone rubber was the major factor influencing the observed stress variation during temperature cycling.

Extensive research has been performed regarding the physical and chemical changes of silicone rubber gasket material in PEMFCs under actual working environments. The focus of the previous

research has been mainly concentrated on gasket performance changes under typical PEMFC operation temperatures (mainly from 60 °C to 80 °C). However, little research has been reported with a focus on the cold start process. The requirement of cold start temperatures is continually being reduced, and the cold start target in Europe has been reduced to -25 °C for fuel cell development scenarios from 2015 to 2020 [34]. Therefore, the degradation of silicone rubber gaskets for PEMFC for the cold start process should be studied as it faces restrictions due to the material property requirements of proton exchange membranes for optimal proton conduction and current formation. In addition, the operating temperature of PEMFC is usually maintained at approximately 80 °C [35]. To decrease the burden of water and heat mass management, increased operating temperature has been targeted for high performance PEMFCs [36-39]. This would be beneficial for water management in PEMFCs as the saturated water vapor pressure increases at higher operating temperatures, resulting in less supersaturated steam inside the PEMFC. This type of research has been pursued by companies such as General Motors, Toyota, and Hyundai as the majority of proton exchange membrane systems currently operate at 80–90 °C [40,41].

To study changes in sealing materials from cold start to normal operation of PEMFCs, a previous study focused on the degradation of silicone rubbers under alternating temperature cycling from −20 °C (cold start) to 90 °C (working temperature) in the presence of de-ionized water and air. The degradation of silicone rubbers was more severe with increasing acid concentration and progressive cycling [42]. In this study, the effect of different cold-start temperatures on the degradation of silicone rubbers was examined and the underlying degradations mechanisms in an actual PEMFC environment are proposed. The degradation of silicone rubbers was investigated using temperature cycling from -5 °C to 90 °C; -10 °C to 90 °C; and -20 °C to 90 °C. Before the silicone rubber degradation experiment, solutions similar to the actual PEM fuel cell environment were prepared [24, 43]. To obtain a better comparison of silicone rubber degradation, the weight and hardness of the silicone rubber were analyzed before the experiment and at predetermined temperature cycles. Atomic absorption spectrometry (AAS) was used to identify the chemicals leached from the silicone rubber into the simulated PEMFC solution. In addition, topographical changes on the surface of the tested samples were examined using scanning electron microscopy (SEM). The chemical changes of the silicone rubber were further examined by attenuated total reflection Fourier transform infrared (ATR-FTIR) spectroscopy. Finally, the aged silicone rubbers were cut into seal rings and assembled into a single cell to study gas leakage in detail. The sealing performances of the aged silicone rubber samples in PEMFCs were determined and compared. This study was performed to establish a degradation mechanism of PEMFC sealing materials during the cold start process to better predict the service life of PEMFC components and rubber sealant performance.

2. EXPERIMENTAL

2.1. Test material and environments

Herein, the investigated methylvinyl silicone rubbers with hardness and thickness values of 50 (Shore A) and 0.5 mm, respectively, were provided by Silicone Rubber Products Co. Ltd (China). The silicone rubber samples were uniformly cut into squares with lengths of 10.0 cm and widths of 4.0 cm.

De-ionized water was used for solution preparation with a resistivity of 18.0 M Ω cm^{-1} produced using a Milli-Q system (Barnsted Nanopore). A pH 3.35 solution, consistent with an actual PEMFC operating environment, with a chemical composition of 12 ppm H_2SO_4 and 1.8 ppm HF was used.

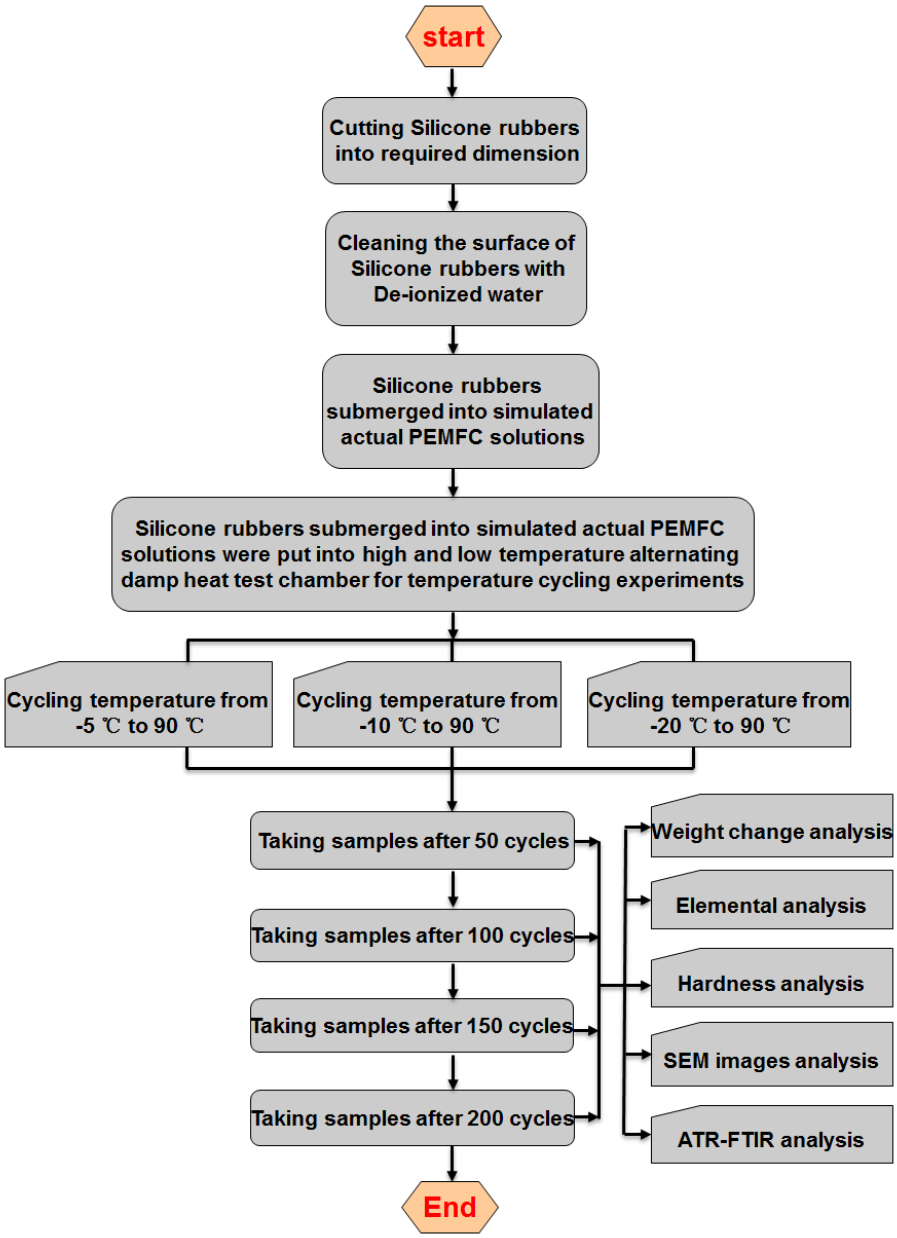

Figure 1. Silicone rubbers aging test process

All silicone rubber samples exposed to the simulated PEMFC operating environment solution were placed in a temperature cycle test chamber (Wuxi Zhuo Cheng Test Equipment Co., Ltd., China) for the alternating temperature cycling experiment. The experimental process is described schematically in Figure 1.

2.2. The cold-start process and characterization methods

Before alternating temperature cycling, the silicone rubber samples were rinsed with de-ionized water to clean their surfaces. Three groups of silicone rubber samples were then submerged into the prepared solutions in three separate containers and subsequently were placed in high and low temperature alternating damp heat test chambers for the cold-start experiment. The experiments were conducted from -5 to 90 °C; -10 to 90 °C; and -20 to 90 °C, which is considered a single temperature cycle, lasting for 3.5, 4.5 and 6 h, respectively. The degraded silicone rubbers were removed from the temperature cycle test chamber every 50 cycles, thoroughly flushed with de-ionized water and dried in air for further analysis. A total of 200 temperature cycles were performed for all the silicone rubber samples. The cumulative running times of the three temperature cycles were 700, 900, and 1200 h, respectively.

Every 50 alternating temperature cycles, the weight of each silicone rubber sample was measured using a microelectronic balance. Before weighing, the silicone rubber samples were rinsed with 18 MΩ cm^{-1} deionized water, followed by air-drying at room temperature, which lasted for >2 h. The hardness of the silicone rubber samples was measured using a Shore A durometer following the ASTM D 2240 standard. The applied test pressure was sufficient to ensure close contact of the durometer with the test samples, and the hardness was recorded immediately after close contact was established. To prevent errors caused by fatigue effects, the test samples were shifted to a new position after each contact. The solutions in which the samples were submerged were analyzed using an atomic absorption spectrometer (Australia GBC AVANTA M) every 50 cycles. The surface morphology of the aged silicone rubbers was examined by scanning electron microscopy (SEM; JEOL JSM-5610LV). Attenuated Total reflection Fourier transform infrared spectra (ATR-FTIR; Bio- Rad FTS 300) with a resolution of 4 cm^{-1} was used to investigate the chemical degradation of silicone rubbers.

2.3 PEMFC gas leakage experiment

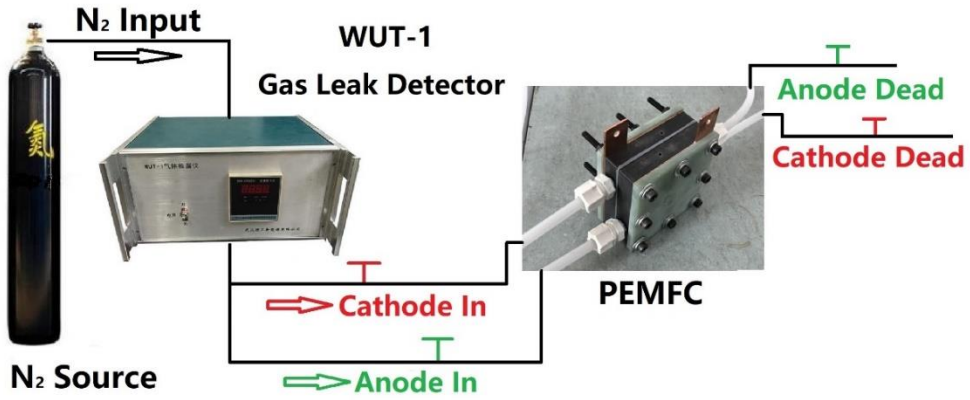

Figure 2. Schematic diagram of PEMFC gas leakage test

After 50 alternating temperature cycles, the aged silicone rubber samples were cut into gaskets with width of 2.5 mm and assembled in a PEMFC single cell with an active area of 4 cm^2 for the gas leakage test (Figure 2).

Nitrogen was supplied to the anode or cathode inlet at a preset pressure using a gas leak detector (WUT-1) located in the outlet of the nitrogen cylinder. Four solenoid valves were equipped to the two inlets and two outlets of the single cell. During the gas leakage experiment, an inlet solenoid valve was opened, and the other three solenoid valves remained closed. The gas leak detector installed in front of the open inlet solenoid valve monitored gas leakage. To analyze the effect of gas pressure on gas leakage, the nitrogen inlet absolute pressure was set to 150, 200, 250, and 300 kPa. To further study the effects of the compression rate of the silicone rubbers on gas leakage, the compression rates of the silicone rubbers assembled in the single cell were set to 15%, 20%, 25%, and 30%.

3. RESULTS AND DISCUSSION

3.1 Silicone rubber weight changes

The silicone rubber samples experiencing the cold-start process were removed from the test chamber after every 50 alternating temperature cycles for weighing. The changes were calculated using the following equation:

$$W(\%) = \frac{W_N - W_0}{W_0} \times 100\% \qquad (1)$$

where W_0 and W_N are the weights of the new samples and the sample after N temperature cycles, respectively.

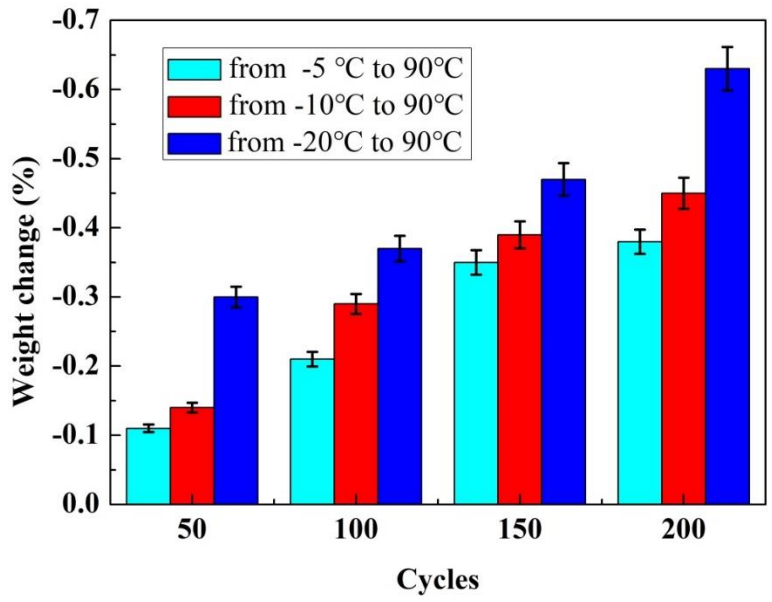

Figure 3. Weight change of the of the silicone rubbers

Figure 3 shows the weight change of the silicone rubbers in the PEMFC environment under different cold-start processes. It is evident that weight loss occurred in all silicone rubber samples during the cold-start process, where the weight loss increased as the initial cold-start temperature decreased from -5 °C to -20 °C, reflecting a wider circulating temperature range. Wider ranges of circulating temperatures used in the experiment resulted in increased weight loss of the silicone rubber. Typically, fillers including silicon dioxide and calcium carbonate are impregnated into the silicone rubber to improving its mechanical properties [9]. When silicone rubber was exposed to the PEMFC operating environment combined with cold-start processes, the silicone rubber experienced thermal expansion and contraction, causing the polysiloxane backbone to swell and leach fillers, resulting in weight loss [25]. Under these conditions, the release of cyclic siloxanes contributed to the majority of the observed weight loss [15]. Thus, the silicone rubber sample weight loss at lower initial cycling temperatures was more pronounced due to the severe expansion and contraction. In addition, the number of alternating temperature cycles and the range of circulating temperatures significantly affected sample weight loss when exposed to the simulated PEMFC environment.

3.2 Atomic absorption spectrometry

Fillers impregnated into the silicone rubbers to improve their mechanical properties can leach into the soaking solution during the cold-start process. To further study this phenomenon, AAS was used to analyze the soaking solution atomic composition.

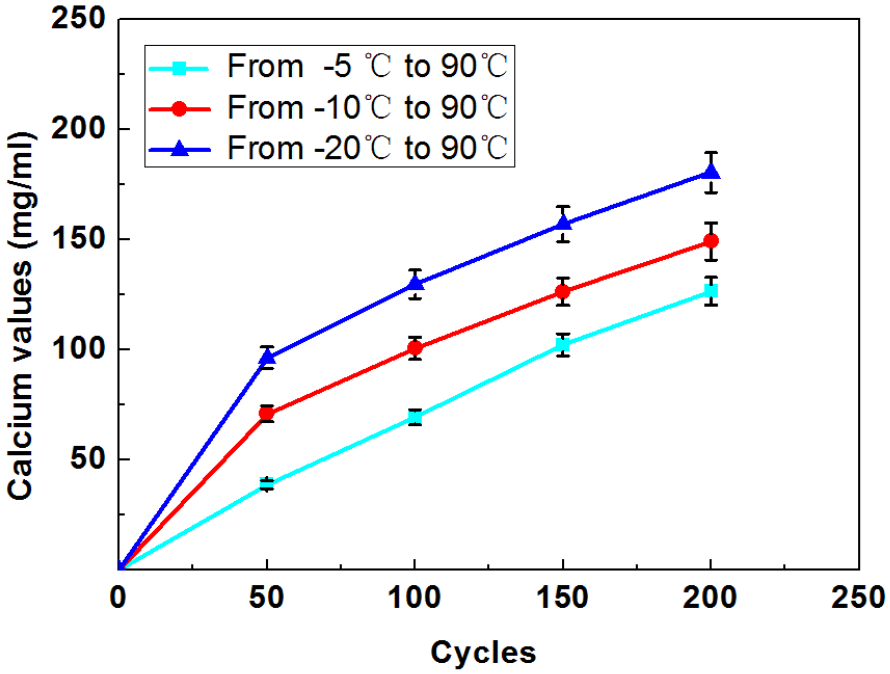

Figure 4. Change of calcium concentration

Figure 4 shows the calcium concentrations of the solution in which the sample was immersed under different alternating temperature cycling regimes. It is clear that the concentration of the leaching chemicals increased with successive alternating temperature cycles. The rate of increase slowed gradually with progressive cycling number. Of all alternating temperature cycles tested herein, lower initial cycling temperatures resulted in higher calcium concentrations in the solutions.

During the temperature cycling, the silicone rubbers suffered from chemical attack by the acidic solutions as well as thermal expansion and contraction. Fillers such as calcium carbonate can be dissolved by the acidic PEMFC environment [9]. The identification of leaching chemicals in the soaking solution indicates that these elastomeric gasket materials degraded in the PEMFC environment.

3.3 Shore A hardness change

The Shore A hardness of the silicone rubbers experiencing cold-start processes were analyzed every 50 alternating temperature cycles using Shore A durometer, as shown in Figure 5. The Shore A hardness of all the silicone rubber samples generally increased, indicating that the surface layers of the aged silicone rubbers hardened with alternating temperature cycling. The Shore A hardness of the samples cycled at lower initial temperatures increased more slowly than those cycled at higher initial temperatures.

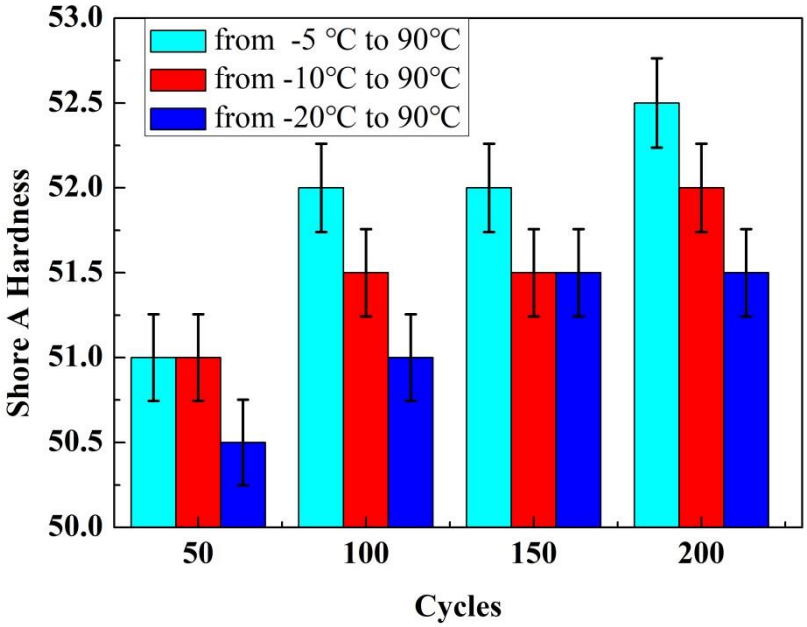

Figure 5. Hardness change of the silicone rubbers

With decreasing initial cycle temperature, molecular activity was reduced. The activities of the side groups, chains, and segments in the silicone rubber became increasingly reduced, causing the rubber to shrink. As the cycling temperature was gradually increased to 90 °C, the filler leached out by thermal expansion and contraction combined with the reaction with the acidic solution. At lower initial

temperatures, greater contraction of the silicone rubber was observed which caused increased filler leaching and resulted in reduced hardness of the samples. However, the rubber samples became prone to cross-linking under altering temperature cycling [44-46]. Thus, the hardness of the aged silicone rubbers surface increased with progressive alternating temperature cycles because the polymer chains could not explore different configurations and became less flexible [42]. Therefore, the Shore A hardness of the silicone rubbers cycled from -20 °C to 90 °C increased more slowly compared to those of the silicone rubbers cycled under temperature regimes with higher initial cold-start temperatures.

3.4 Surface SEM analysis

Figure 6 shows the surface morphology changes of the silicone rubber samples subjected to different cold-start process. The surface was rather smooth and no voids or cracks were observed in the original silicone rubber (Fig. 6(a)).

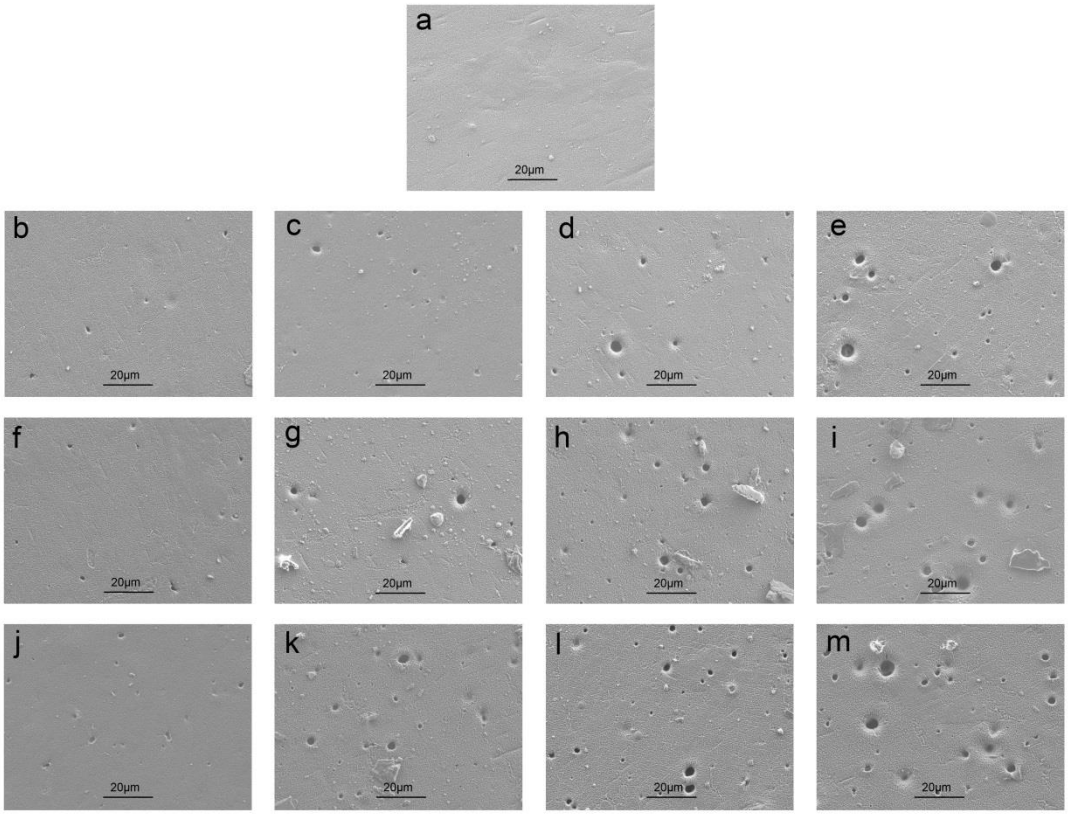

Figure 6. SEM images of silicone rubbers under different temperature cycling (a) original, (b) 50 cycles from -5 °C to 90 °C, (c) 100 cycles from -5 °C to 90 °C, (d) 150 cycles from 5 °C to 90 °C, (e) 200 cycles from -5 °C to 90 °C, (f) 50 cycles from -10 °C to 90 °C, (g) 100 cycles from -10 °C to 90 °C, (h) 150 cycles from -10 °C to 90 °C, (i) 200 cycles from -10 °C to 90 °C, (j) 50 cycles from -20 °C to 90 °C, (k) 100 cycles from -20 °C to 90 °C, (l) 150 cycles from -20 °C to 90 °C, (m) 200 cycles from -20 °C to 90 °C.

Figure 6b–e shows the surface topographical changes of the aged silicone rubber after 50, 100, 150, and 200 cycles, respectively, with an alternating temperature from -5 °C to 90 °C. Some voids or

cracks formed on the surface of the samples after 50 cycles and these voids and cracks continuously grew with increasing number of cycles. These voids and cracks appeared to be the same with other results that the degradation of silicon rubber started from surface roughness and finally cracks exhibited temperature gradient dependent as well as time-dependent [11, 14, 18, 19, 32].

Figure 6f–i shows the morphological changes of the silicone rubber surface after alternating temperature cycles from -10 °C to 90 °C. Figure 6j–m shows the morphological changes of the silicone rubber surface after cycling from -20 °C to 90 °C. With decreasing cold-start initial temperature, voids and cracks became larger and more abundant, and holes and cracks were observed under the same alternating temperature cycles. Thus, it can be concluded from the SEM results that the silicone rubber surface damage under PEMFC conditions is more extensive at lower cold-start initial temperatures, and the degradation becomes more severe with progressive temperature cycling [18].

3.5 ATR-FTIR

The ATR-FTIR spectra of silicone rubber samples subjected to different cold-start process are shown in Figure 7. The strongest and broadest absorption band was observed between 1010 and 1080 cm^{-1}, with other prominent absorption bands at 793, 864, 1260, and 2962 cm^{-1}, respectively.

For the three cold-start processes tested herein, the intensity of the bands remained largely unchanged after 50 cycles (Figs. 7(a)). This indicates that the surface chemistry of the silicone rubber did not change at a small cumulative cycle number. As the number of cycles was increased to 100, the intensity of the bands did not change in silicone rubber samples cycled from -5 °C to 90 °C (Fig. 7(b)). However, the intensity of the absorption band at 1080 cm^{-1} decreased slightly in the sample cycled from -10 °C to 90 °C, and decreased significantly in those cycled from -20 °C to 90 °C.

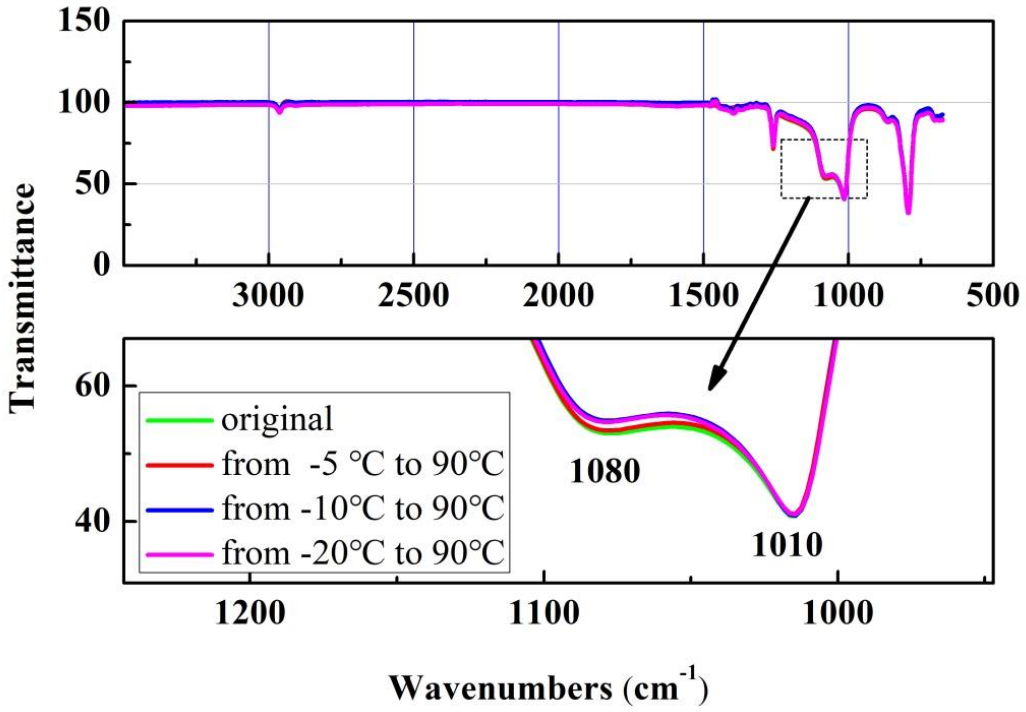

(a)

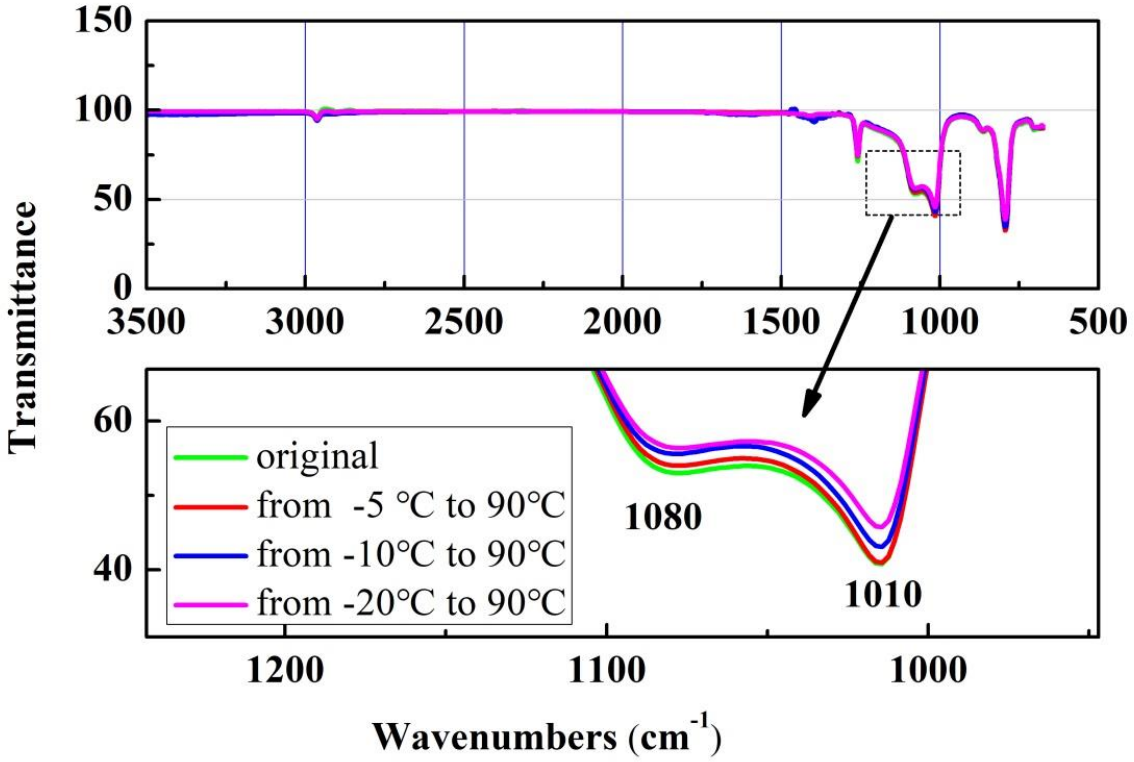
Transmittance
150
100
50
0
3500
3000
2500
2000
1500
1000
500
60
40
original
from -5 °C to 90°C
from -10°C to 90°C
from -20°C to 90°C
1080
1010
1200
1100
1000
Wavenumbers (cm-1)

(b)

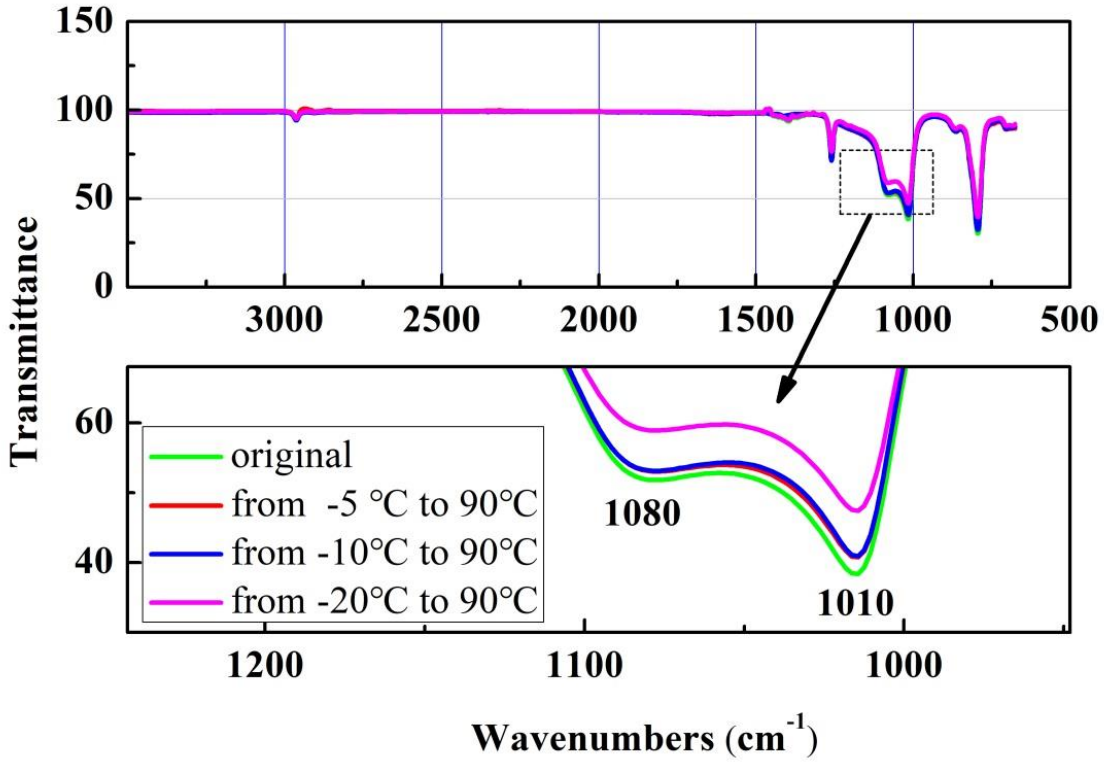
Transmittance
150
100
50
0
3000
2500
2000
1500
1000
500
60
40
original
from -5 °C to 90°C
from -10°C to 90°C
from -20°C to 90°C
1080
1010
1200
1100
1000
Wavenumbers (cm-1)

(c)

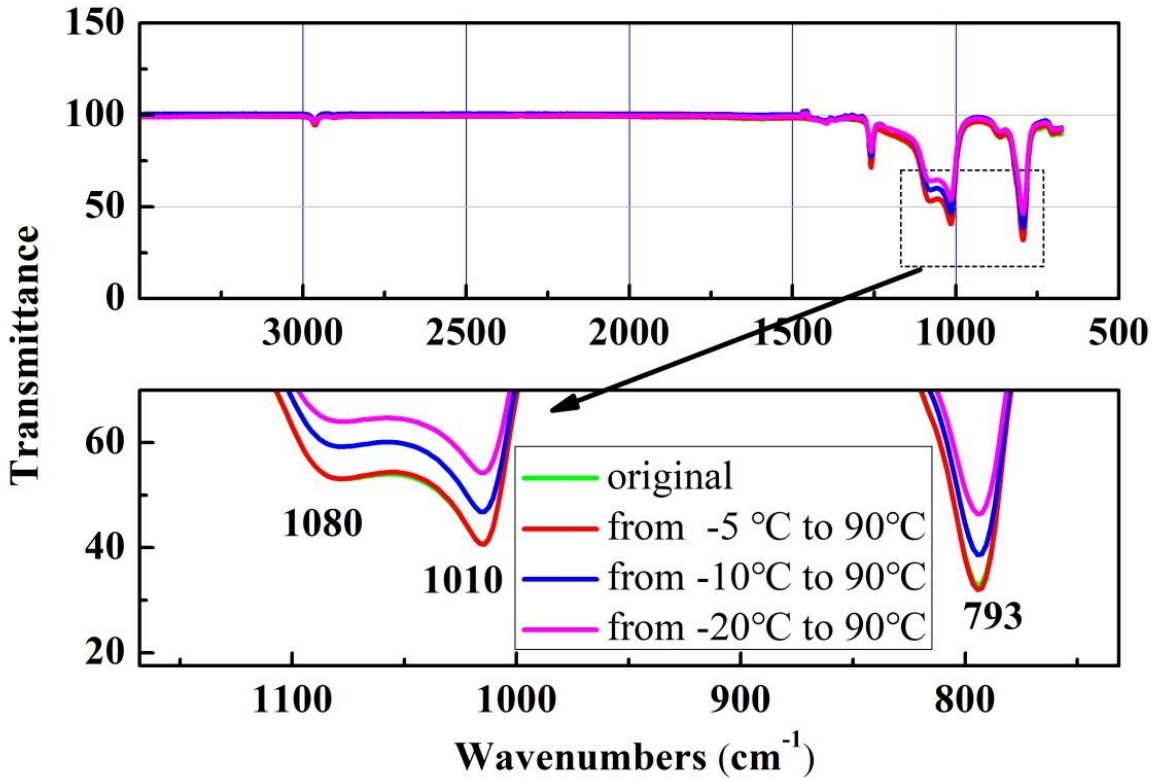

(d)

Figure 7. ATR-FTIR spectra of silicone rubbers under different temperature cycling(a) 50 temperature cycles, (b) 100 temperature cycles, (c) 150 temperature cycles, (d) 200 temperature cycles

After 150 cycles, the intensity of the absorption bands showed no obvious changes for the samples cycled from -5 °C to 90 °C. For the lower initial temperature cycles, the intensity of the absorption bands between 1010 and 1080 cm^{-1} decreased more sharply compared to that of the samples analyzed after 100 temperature cycles. At an initial temperature of -20 °C, the intensity of the absorption band at 1080 cm^{-1} decreased significantly, while the intensity of the other peaks remained largely unchanged. After 200 cycles, the absorption band intensities were unchanged in the silicone rubber cycled from -5 °C to 90 °C (Fig. 7(d)). However, the intensity of the absorption bands at 1010, 1080, and 793 cm^{-1} decreased dramatically for the other two cycling regimes. The intensity of the absorption bands at the peak values was changed at cold start conditions, which could be seen at other conditions such as accelerated PEM fuel cell environment at constant temperature and PEM fuel cell environment at different cycle temperature [18, 19, 30, 32, 33], which indicated that the same chemical changes had taken place on the aging surface of silicone rubber.

Briefly, the intensity of all absorption bands of the silicone rubber samples in the PEMFC environment under temperature cycling from -5 °C to 90 °C showed no significant changes. However, decreasing initial cold-start temperature resulted in changes in the intensity of the absorption bands. These results show that the number of cycles and initial temperature of the cycles significantly affected the degradation of the tested silicone rubbers.

3.6 Sealing performance of the aged silicone rubbers

The sealing performance of the aged silicone rubbers as gaskets for a PEMFC single cell with an active area of 4 cm^2 was investigated by gas leakage tests. The compression rates of the gaskets assembled in the single cell were 15%, 20%, 25%, and 30%.

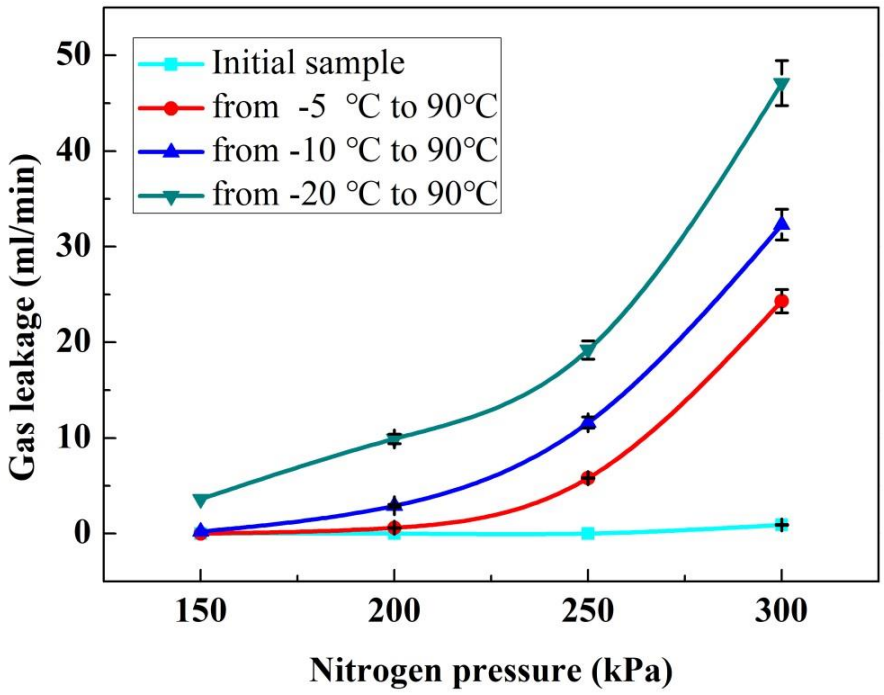

(a)

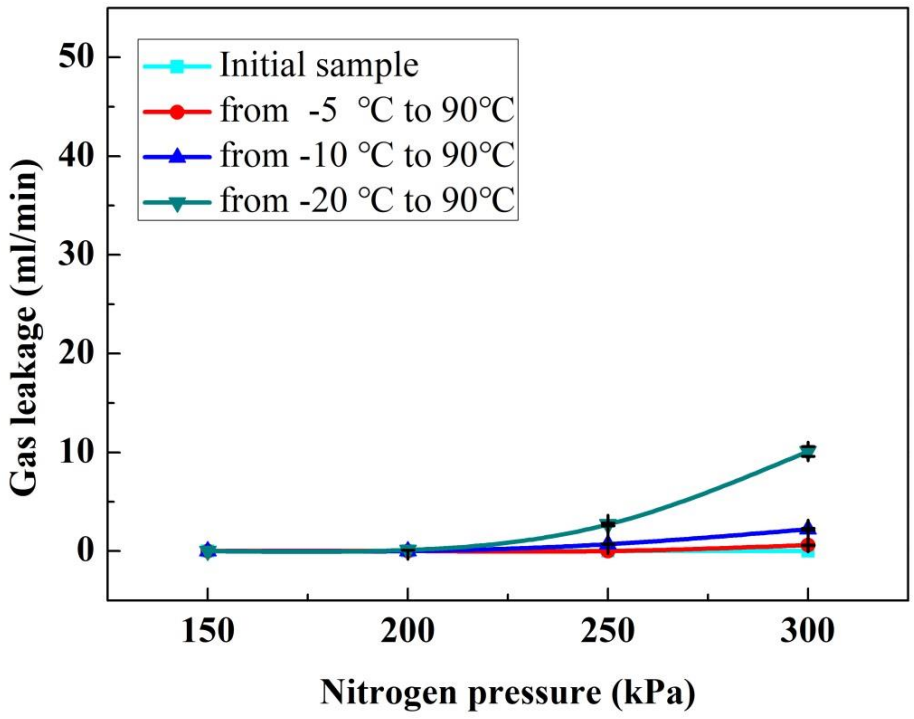

(b)

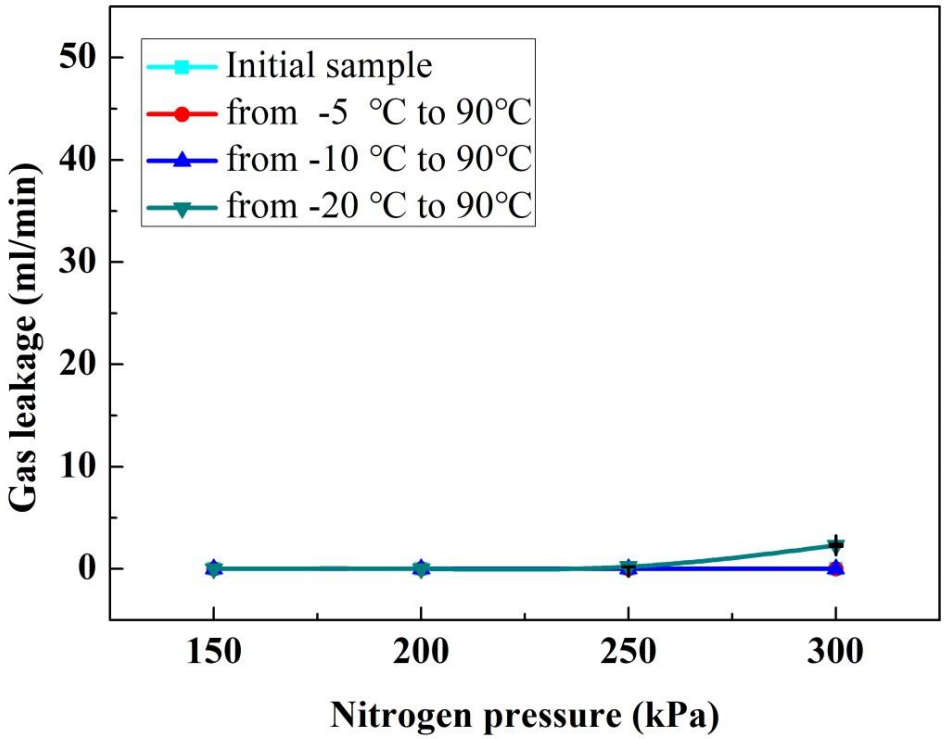

(c)

Figure 8. Gas leakages of the aging silicone rubbers at 15% (a), 20% (b) and 25% (c) compression rate as gasket assembled in single cell

Figure 8 shows the gas leakage of the assembled single cell under the different compression rates. A noticeable gas leakage was observed in the single cell at a lower compression rate, especially under high nitrogen inlet pressure. At a compression rate of 15% and under a nitrogen inlet pressure of 300 kPa, gas leakage rates were 24.3, 31.8, and 47.2 mL/min under temperature cycling from -5 °C to 90 °C; -10 °C to 90 °C; and -20 °C to 90 °C, respectively. It is referred to the regulations of the United States, Europe and Japan on hydrogen leakage and hydrogen emission of fuel cell vehicles that these leakage rates are excessively severe for a PEMFC with an active area of 4 cm^2, and the sealing performance was judged to be near failure [47]. However, for the pristine silicone rubber samples, negligible gas leakage was observed. Thus, the sealing performance of the aged silicone rubber obviously declined.

As the compression rate of the gaskets was increased to 20%, gas leakage was significantly reduced to 10.4 mL/min under alternating temperatures from -20 °C to 90 °C, while almost no change was observed under other temperature cycling regimes with higher initial temperatures. As the compression rate of the gaskets was increased to 25% and 30%, no gas leakage was observed. Thus, the sealing performance of the silicone rubbers was partially degraded after aging, especially at higher gas pressures, low compression rates, and lower initial cold-start cycling temperatures. These results indicate that the cold-start process of PEMFC can significantly influence the sealing performance of silicone rubber.

4. CONCLUSIONS

The degradation properties of silicone rubbers as potential gasket materials for PEMFCs were investigated in different cold-start processes, with cycling from -5 °C to 90 °C; -10 °C to 90 °C; and -20 °C to 90 °C. The major conclusions of this study are as follows:

(1) The initial cold-start cycle temperature and the number of temperature cycles significantly affected the degradation of silicone rubbers, as evidenced by the sample weight loss. Weight loss was more significant at lower initial cold-start cycling temperatures and with progressive temperature cycles, which was corroborated by AAS measurements.

(2) The silicone rubbers exhibited a slight increase in hardness, indicating severe damage of the fillers in the silicone rubbers at lower initial temperatures compared to that at higher initial temperatures. SEM images indicated that the degradation began via formation of surface holes and progressive formation of larger voids.

(3) ATR-FTIR spectrometry revealed that after the cold-start process, the surface chemistry of the silicone rubbers had significantly altered.

(4) The sealing performance of the silicone rubbers was partially degraded after 200 temperature alternating cycles. After aging, a high compression rate can maintain the sealing performance of silicone rubbers.

The current study demonstrates the effects of the cold-start process on the degradation of silicone rubber material. The mechanical performance of the aged silicone rubber was degraded, resulting in poor sealing performance. This study provides guidance for future work dedicated to improving the durability and reliability of silicone rubbers as sealants for PEMFCs in the context of cold-start processes.

ACKNOWLEDGEMENTS
This work was supported by the National Natural Science Foundation of China (Nos. 51706162 and 51776144) and the Fundamental Research Funds for the Central Universities (No. 2018 IVB 063).

References

1. J. Shen, Z.K. Tu, S. H. Chan, *Appl. Therm. Eng.,* 149 (2019) 1408-1418.
2. H.W. Chang, C. Duan, X.X. Xu, S.M. Shu, Z.K. Tu, *Int. J. Hydrogen Energy,* 44 (2019) 21080-21089.
3. S. Srinivasan. *Fuel cells: from fundamentals to applications*, Springer, New York, 2006.
4. Z.H. Wan, Q. Zhong, S.F. Liu, A.P. Jin, Y.N. Chen, J.T. Tan, M. Pan, *Int. J. Energy Res.,* 42 (2018) 2225-2233.
5. F.A. de Bruijn, V.A.T. Dam, G.J.M. Janssen, *Fuel Cells,* 8 (2008) 3-22.
6. Y. Luo, K. Jiao, *Prog. Energy Combust. Sci.*, 64 (2018) 29-61.
7. O. Gröger, H.A. Gasteiger, J. P. Suchsland, *J. Electrochem. Soc.,* 162 (2015) A2605-A2622.
8. T. Cui, C.W. Lin, C.H. Chien, Y.J. Chao, J.W. Van Zee, *J. Power Sources,* 196 (2011) 1216-1221.
9. K.D. Baik, I.M. Kong, B.K. Hong, S.H. Kim, M.S. Kim, *Appl. Energy,* 101 (2013) 560-566.
10. U. Chakraborty, *Appl. Energy,* 163 (2016) 60-62.
11. C.W. Lin, C.H. Chien, J. Tan, Y.J. Chao, J.W. Van Zee, *J. Power Sources,* 196 (2011) 1955-1966.
12. S.J.C. Cleghorn, D.K. Mayfield, D.A. Moore, J.C. Moore, G. Rusch, T.W. Sherman, N.T. Sisofo, U. Beuscher, *J. Power Sources,* 158 (2006) 446-454.
13. X. Li, Y.H. An, Y.D. Wu, Y.C. Song, Y.J. Chao, C.H. Chien, *J. Biomed. Mater. Res. Part B,* 80B (2007) 25-31.

14. T. Cui, Y.J. Chao, X.M. Chen, J.W. Van Zee, *J. Power Sources*, 196 (2011) 9536-9543.
15. S. Bhargava, K.A. O'Leary, T.C. Jackson, B. Lakshmanan, *Rubber Chem. Technol.*, 86 (2013) 28-37.
16. D.A. Dillard, S. Guo, M.W. Ellis, J.J. Lesko, J.G. Dillard, J. Sayre, B. Vijayendran, *ASME 2004 2nd Int. Conf. Fuel Cell Sci.*, 01(2004) 01.
17. M.S. Kim, A.H. Kim, J.K. Kim, S.J. Kim, *Macromol. Res.*, 15 (2007) 315-323.
18. G. Li, J. Tan, J. Gong, *J. Power Sources*, 205 (2012) 244-251.
19. G. Li, J. Tan, J. Gong, *J. Power Sources*, 217 (2012) 175-183.
20. J.K. Kim, I.H. Kim., *J. Appl. Polym. Sci.*, 79 (2001) 2251-2257.
21. D. Graiver, K.W. Farminer, R. Narayan, *J. Polym. Environ.*, 11 (2003) 129-136.
22. D.E. Curtin, R.D. Lousenberg, T.J. Henry, P.C. Tangeman, M.E. Tisack, *J. Power Sources*, 131 (2004) 41-48.
23. B. Marungsri, H. Shinokubo, R. Matsuoka, S. Kumagai, *IEEE Trans. Dielectr. Electr. Insul.*, 13 (2006) 129-138.
24. H.W. Chang, Z.M. Wan, X. Chen, J. Wan, L. Luo, H.N. Zhang, S. Shu, Z.K. Tu, *Appl. Therm. Eng.*, 104 (2016) 472-478.
25. J. Feng, Q. Zhang, Z.K. Tu, W.M. Tu, Z.M. Wan, M. Pan, H.N. Zhang, *Polym. Degrad. Stab.*, 109 (2014) 122-128.
26. J. Tan, Y.J. Chao, X. Li, J.W. Van Zee, *J. Power Sources*, 172 (2007) 782-789.
27. J. Tan, Y.J. Chao, J.W. Van Zee, W.K. Lee, *Mater. Sci. Eng. A*, 445 (2007) 669-675.
28. J. Tan, Y.J. Chao, M. Yang, C.T. Williams, J.W. Van Zee, *J. Mater. Eng. Perform.*, 17 (2008) 785-792.
29. J. Tan, Y.J. Chao, X. Li, J.W. Van Zee, *J. Fuel Cell Sci. Technol.*, 6 (2009) 041017.
30. J. Tan, Y.J. Chao, M. Yang, W.-K. Lee, J.W. Van Zee, *Int. J. Hydrogen Energy*, 36 (2011) 1846-1852.
31. S. Pehlivan-Davis, J. Clarke, S. Armour, *J. Appl. Polym. Sci.*, 129 (2013) 1446-1464.
32. T. Cui, Y.J. Chao, J.W. Van Zee, *Polym. Test.*, 32 (2013) 1202-1208.
33. T. Cui, Y.J. Chao, J.W. Van Zee, *Int. J. Hydrogen Energy*, 39 (2014) 1430-1438.
34. 2011 Annual implementation plan of fuel cells and hydrogen joint undertaking [Accessed on 1-Oct-2017]
35. Z.K. Tu, H.N. Zhang, Z.P. Luo, J. Liu, Z.M. Wan, M. Pan, *J.Power Sources*, 222 (2013) 277-281.
36. M.F. Torchio, M.G. Santarelli, A. Nicali, *J. Power Sources*, 149 (2005) 33-43.
37. J. Zhang, Z. Xie, J. Zhang, Y. Tang, C. Song, T. Navessin, Z. Shi, D. Song, H. Wang, D.P. Wilkinson, Z. S. Liu. S. Holdcroft, *J. Power Sources*, 160 (2006) 872-891.
38. M. Chahartaghi, B.A. Kharkeshi, *Appl. Therm. Eng.*, 128 (2018) 805-817.
39. L. Barelli, G. Bidini, F. Gallorini, A. Ottaviano, *Appl. Energy*, 91 (2012) 13-28.
40. V. P Mcconnell, *Fuel Cells*, 12 (2009) 12-16.
41. W. Wu, *Shanghai Auto*, 9 (2014) 29-33.
42. F. Wu, B. Chen, Y.Z. Yan, Y.N. Chen, M. Pan. *Polymers*, 10 (2018) 522.
43. C.W. Lin, C.H. Chien, J. Tan, Y.J. Chao, J.W. Van Zee, *Int. J. Hydrogen Energy*, 36 (2011) 6756-6767.
44. N. Yoshimura, *IEEE Trans. Dielectr. Electr. Insul.*, 6 (1999) 632-650.
45. Y.W. Bao, W. Wang, Y.C. Zhou, *Acta Mater.*, 52 (2004) 5397-5404.
46. F. Delor-Jestin, N.S. Tomer, R.P. Singh, J. Lacoste, *e-polymers*, 013 (2006) 1-13.
47. H. Gao, C. Zhang, K. Qin, *Shanghai Auto*, 6 (2008) 11-13.